Progress In Electromagnetics Research M, Vol. 17, 59–71, 2011

ACCURATE MODELING OF COUPLING JUNCTIONS IN DIELECTRIC COVERED WAVEGUIDE SLOT ARRAYS

G. Mazzarella and G. Montisci

Dipartimento di Ingegneria Elettrica ed Elettronica
Univ. di Cagliari, Piazza D'Armi, Cagliari 09123, Italy

Abstract—This paper investigates the higher-order modes interaction between a coupling slot and the radiating ones in a dielectric-covered waveguide slot array environment. This interaction can strongly affect the array aperture distribution and input match, mainly when each radiating guide contains few slots or the slots offsets are small. We propose a full-wave Method of Moments approach, taking also into account the waveguide wall thickness, to evaluate this interaction. The use of entire domain basis functions allows to get a small and well-conditioned linear system. The results presented in this paper show that the coupling due to higher-order modes in the region of the junction can significantly modify the array aperture distribution, mainly when the offset is small, and also the array input match, though to a lesser extent.

1. INTRODUCTION

Waveguide-fed slot arrays were proposed many decades ago as microwave antennas for radar and communication systems but are still widely in use today for their advantages. Among them, we remember here their high efficiency, which makes them a popular choice in aerospace applications, for operating frequencies up to the millimeter wave band. In such applications the slot array is usually covered with a thin dielectric layer to pressurize the waveguide in order to increase the maximum allowed power, or simply for protection. Clearly this dielectric cover significantly modifies the array behavior.

For arrays radiating into free-space the state of the art is very satisfactory. The design of slot arrays was based on semi-empirical methods until the publication of a paper by Elliot [1] which gave

Received 28 December 2010, Accepted 11 February 2011, Scheduled 14 February 2011
Corresponding author: Giorgio Montisci (giorgiom@diee.unica.it).

a rigorous synthesis procedure, able to fully take into account the external mutual coupling. In Elliott's model, each radiating guide (and feeding one as well) is described by its TE_{10} transmission line, periodically loaded by lumped components, representing radiating slots (or couplers). The external mutual coupling between radiating slots is taken into account in the admittance (which is, actually, an active admittance) of such lumped components. The interaction between the coupling slot and the radiating ones is modeled by using only the TE_{10} mode. Moreover, this TE_{10} interaction is computed assuming that these slots do not overlap, i.e., assuming that a trunk of waveguide without discontinuities (so allowing a modal expansion of the field) exists between the slots. After Elliott, a large number of papers, dealing with the secondary effects neglected in his work, have appeared. For example, just to name a few, in [2] Elliott and O'Loughlin include the internal (TE_{20} mode) coupling between radiating slots in the transmission line model. In [3] Mazzarella and Panariello deal with the edge effects in slot arrays by using the Geometrical Theory of Diffraction, and in [4] Rengarajan and Shaw analyze the higher-order modes interaction between coupling and radiating slots. Taking into account all these second-order effects significantly improves the accuracy and reliability of the design procedure. Therefore, the design of a slot array radiating into free space can be presently done in a reliable and accurate way.

The above scenario, however, is quite different for dielectric-covered arrays, since many of those secondary effects depend on the environment in which the array radiates.

Therefore, inclusion of second-order effects for the dielectric-covered case should be dealt with almost from the beginning. To the best of our knowledge, only a few papers, dealing with the characterization of a single radiating slot, exist (see, e.g., [5, 6] and [7]), and no secondary effects have been considered so far. Among such effects, the higher-order modes interaction between coupling and radiating slots is one of the most important. Actually, it affects both the aperture distribution and the input match, mainly when each branch-guide contains only a few slots. Since it involves radiating slots, the dielectric-covered case is completely different from the free-space case dealt with in [4].

The aim of this paper is to investigate, using a rigorous Method of Moment (MoM) procedure, the interaction of the dielectric-covered radiating slots with a coupling slot cut in the opposite wall of the waveguide. Special care has been put in devising a very effective analysis procedure, so to render the design of the coupling slot, taking this interaction into account, a feasible task. The only simplifying

assumption is a standard one [1, 4, 8], namely that all slots are narrow, so that we can neglect both the longitudinal E-field and the transverse variation of its transverse component. The effect on the input admittance and on the excitation of the radiating slots has been computed to quantitatively evaluate the discrepancies introduced by the higher-order modes interaction in the region of the coupling junction.

2. PROBLEM FORMULATION

Let us consider the basic structure of Figure 1, where a feeding guide feeds a radiating guide through a coupling slot cut in a thick wall. In this guide a number of slots radiate, through a thin dielectric cover of thickness h and dielectric permittivity ε_r, into the space. We assume that the radiating slots are cut into an infinite ground plane. Moreover, we consider the slots narrow enough to assume (following [1]) that only the longitudinal component of the electric field exists on their apertures, and that this component has no transverse variation and depends only on the longitudinal coordinate ξ (Figure 1).

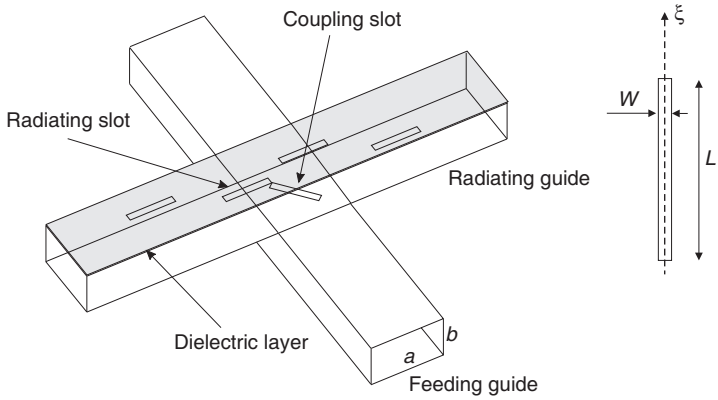

Figure 1. Schematic view of the structure analyzed in the paper and of the slot geometry.

The interaction between the coupling slot and the radiating slots is due to the fundamental TE_{10} mode in the radiating guide, except for the two slots closest to the coupling one. In this case all modes contribute to the interaction, since the distance between the centers of the radiating and coupling slots is $\frac{\lambda_g}{4}$, λ_g being the guide wavelength, and therefore the waveguide sections occupied by the slots overlap (as in Figure 2). According to the equivalence theorem, we can replace

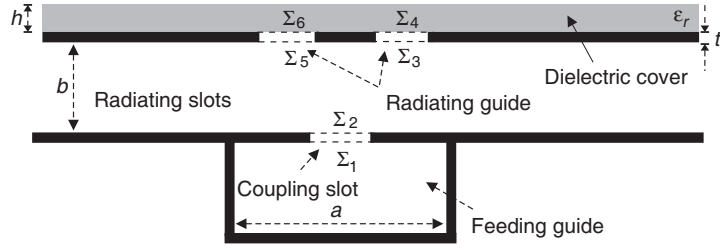

Figure 2. Side view of the structure.

the apertures of all slots (see Figure 2) by conductor-backed magnetic surface currents. Taking into account the thickness of the waveguide walls, we have six unknown currents, which can be all represented as (truncated) Fourier series:

$$\mathbf{M}^k = \sum_{p=1}^{N} a_p^k \sin\left[\frac{p\pi}{L^k}\left(\xi + \frac{L^k}{2}\right)\right]\mathbf{i}_\xi = \sum_{p=1}^{N} a_p^k \mathbf{m}_p^k(\xi) \quad k = 1,\ldots,6 \quad (1)$$

wherein ξ is the longitudinal component on the slot; L^k is the slot length; a_p^k are the unknown expansion coefficients; and k labels the different unknowns on each section Σ^k. We do not include in (1) the Maixner edge condition since the corresponding increase in accuracy is negligible (see [6]) for finite-thickness walls.

In order to compute the unknown coefficients a_p^k, we use the MoM in the Galerkin formulation. We evaluate the magnetic field in each region, impose the continuity condition at each aperture, and get a set of six coupled integral equations:

$$\begin{aligned}
\mathbf{H}_{Sc}[-\mathbf{M}^1,-\mathbf{M}^2] &= \mathbf{H}_F[\mathbf{M}^1] + \mathbf{H}_{inc} && \text{on } \Sigma_1\\
\mathbf{H}_R[\mathbf{M}^2,\mathbf{M}^3,\mathbf{M}^5] &= \mathbf{H}_{Sc}[-\mathbf{M}^1,-\mathbf{M}^2] && \text{on } \Sigma_2\\
\mathbf{H}_{Sr}[-\mathbf{M}^3,-\mathbf{M}^4] &= \mathbf{H}_R[\mathbf{M}^3,\mathbf{M}^2,\mathbf{M}^5] && \text{on } \Sigma_3\\
\mathbf{H}_D[\mathbf{M}^4,\mathbf{M}^6] &= \mathbf{H}_{Sr}[-\mathbf{M}^3,-\mathbf{M}^4] && \text{on } \Sigma_4\\
\mathbf{H}_{Sr}[-\mathbf{M}^5,-\mathbf{M}^6] &= \mathbf{H}_R[\mathbf{M}^3,\mathbf{M}^2,\mathbf{M}^5] && \text{on } \Sigma_5\\
\mathbf{H}_D[\mathbf{M}^4,\mathbf{M}^6] &= \mathbf{H}_{Sr}[-\mathbf{M}^5,-\mathbf{M}^6] && \text{on } \Sigma_6
\end{aligned} \quad (2)$$

wherein $\mathbf{H}_{inc}$ is the magnetic field that impinges upon the coupling slot in the feeding guide; $\mathbf{H}_{Sc}$ is the magnetic field in the coupling slot region; $\mathbf{H}_{Sr}$ is the magnetic field in the radiating slot region; $\mathbf{H}_F$ and $\mathbf{H}_R$ are the magnetic field in the feeding and radiating guides; and $\mathbf{H}_D$ is the magnetic field in the external region.

All equations are then scalar multiplied by $\mathbf{m}_q^k$ to get a linear system in the a_p^k. Since we have used a Fourier series expansion (1), only a few terms of each expansion are needed. The smallness of the resulting linear system and the orthogonality of the basis functions (1) assure that this system is quite well-conditioned. A further improvement to the condition number of the system is obtained using as unknowns $s_p^h = a_p^{2h-1}$ and $d_p^h = \frac{(a_p^{2h} - a_p^{2h-1})}{t}$ with $h = 1, 2, 3$, instead of a_p^{2h-1}, a_p^h, since the values of the latter are very close to each other.

The MoM matrix elements are calculated in the same way as shown in [6, 9] and [10] using the Green function detailed in [6]. It is worth noting, however, that use of (1) as basis functions allows an easy evaluation of the coupling terms between $\mathbf{M}^{2h-1}$ and $\mathbf{M}^{2h}$. Actually, each slot can be seen as a stub waveguide [6], and (1) are its modes, so that the corresponding entries of the MoM matrix are the elements of a 2-by-2 admittance matrix.

3. VALIDATION OF THE METHOD OF MOMENTS PROCEDURE

The proposed MoM analysis procedure has been checked against a commercial Finite Element Method software, Ansoft HFSS. This software is accurate but not very effective for the analysis of waveguide slots, especially for weakly excited radiating slots or reduced waveguide wall thickness. Actually, in these cases, it requires a high number

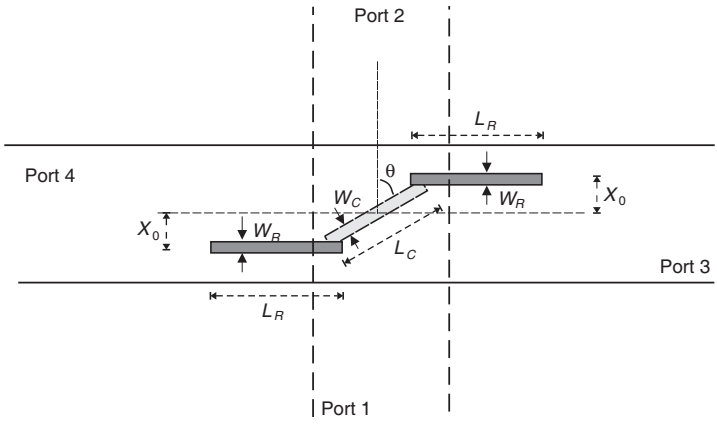

Figure 3. Geometry of the structure under test.

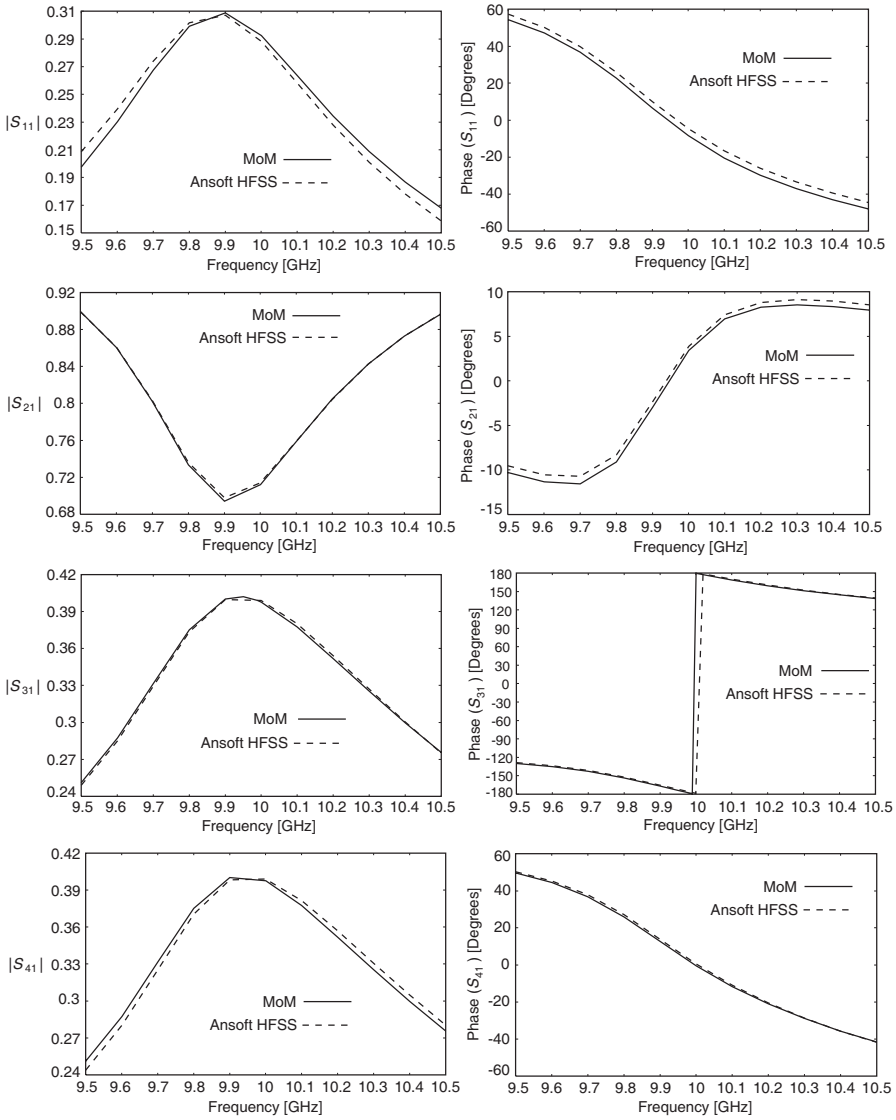

Figure 4. Amplitude and phase of the scattering parameters for the structure in Figure 3. $t = 1.27\,\text{mm}$, $h = 0.165\,\text{mm}$, $\varepsilon_r = 2.05$, $L_R = 14.178\,\text{mm}$, $W_R = 1.58\,\text{mm}$, $X_0 = 4\,\text{mm}$, $L_C = 13.975\,\text{mm}$, $W_C = 3.0\,\text{mm}$, $\theta = 30°$, and both radiating and feeding waveguide are WR90.

of unknowns to converge. Nevertheless, it has been shown that HFSS results are in very good agreement with experiment (see e.g., [11]). Therefore it has been used as a validation tool for our analysis technique.

The geometry of the structure under test is shown in Figure 3 and the comparison between our MoM procedure and Ansoft HFSS results shows a very good agreement (see Figure 4).

4. RESULTS

The pattern of a slot array depends on the distribution of the slot voltages V_S (line integral of the slot electric field at the slot center [1, Equation (2)]). Therefore, its radiating performance can be negatively affected by the higher order modes interaction analyzed here, since the latter modifies the slot voltage distribution w.r.t the design one. The effect of this interaction has therefore been discussed in this section comparing the "correct" value of both the radiating slots voltage V_S and the feeding guide S_{11} (calculated using our full-wave MoM procedure) with the values obtained using the standard circuital model [1] (which includes only the TE_{10} mode interaction). Since an error on V_S degrades the array pattern, and an error on S_{11} affects the antenna input match, such comparison will rate at best the importance of the higher-order modes interaction discussed here.

The main effect of the higher-order modes interaction between a coupling and a radiating slot is a quite strong modification of the radiating slot excitation. The new value of the slot voltage depends on the slot offset, and on the relative orientation of the radiating and coupling slots (soft and hard orientation, according to the notation of [4]), as shown in Figure 5.

In Figures 6 and 7 the slot voltage error is shown, for both orientations and for the interaction of two radiating slots with a coupling one in WR90 waveguides ($a = 22.86\,\text{mm}$, $b = 10.16\,\text{mm}$).

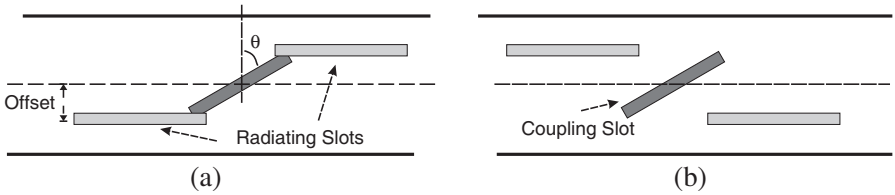

Figure 5. Definition of the (a) "hard" coupling orientation and (b) "soft" coupling orientation.

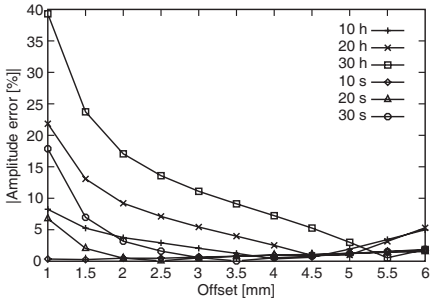

Figure 6. Amplitude error on the slot voltage for standard WR90 waveguides. $t = 1.27\,\text{mm}$; $h = 0.165\,\text{mm}$, $\varepsilon_r = 2.05$.

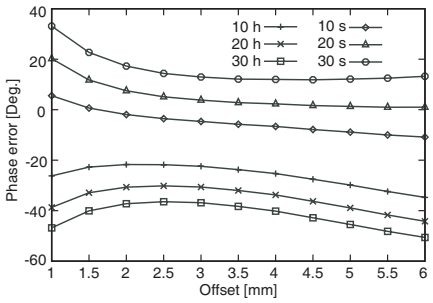

Figure 7. Phase error on the slot voltage for standard WR90 waveguides. $t = 1.27\,\text{mm}$; $h = 0.165\,\text{mm}$, $\varepsilon_r = 2.05$.

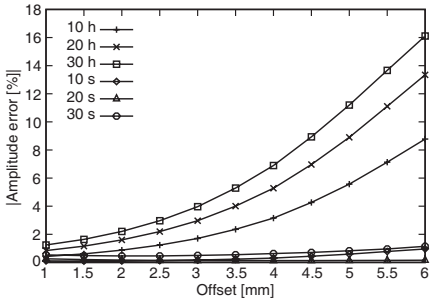

Figure 8. S_{11} amplitude error for standard WR90 waveguides. $t = 1.27\,\text{mm}$; $h = 0.165\,\text{mm}$, $\varepsilon_r = 2.05$.

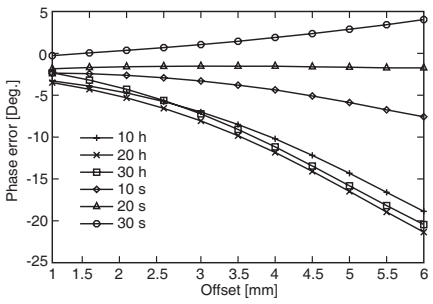

Figure 9. S_{11} phase error for standard WR90 waveguides. $t = 1.27\,\text{mm}$; $h = 0.165\,\text{mm}$, $\varepsilon_r = 2.05$.

The thickness of the dielectric cover is $h = 0.165\,\text{mm}$, and its dielectric permittivity is $\varepsilon_r = 2.05$. The coupling slot length is chosen in order to make it resonant at 10 GHz at the chosen tilt angle, while its width is $W_C = 3.0\,\text{mm}$. The radiating slot centers are spaced $\frac{\lambda_g}{2}$; their length are chosen in order to make them resonant at 10 GHz (when isolated); and their width is $W_R = 1.58\,\text{mm}$. We consider different coupling slot tilt angles θ, marked with hard and soft orientation, designated by "h" and "s" respectively (Figure 5). In order to evaluate the effect of the higher-order modes interaction on the coupling slot, in Figures 8 and 9 we also show the error in the S_{11} scattering parameter. The effect is larger for the hard case and mainly for the radiating slot voltage rather than for the S_{11}.

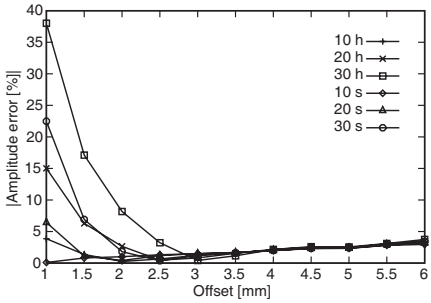

Figure 10. Amplitude error on the slot voltage for half-height WR90 waveguides. $t = 1.27\,\text{mm}$; $h = 0.165\,\text{mm}$, $\varepsilon_r = 2.05$.

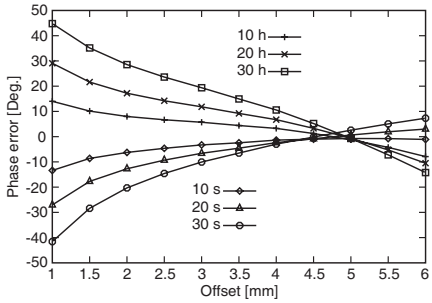

Figure 11. Phase error on the slot voltage for half-height WR90 waveguides. $t = 1.27\,\text{mm}$; $h = 0.165\,\text{mm}$, $\varepsilon_r = 2.05$.

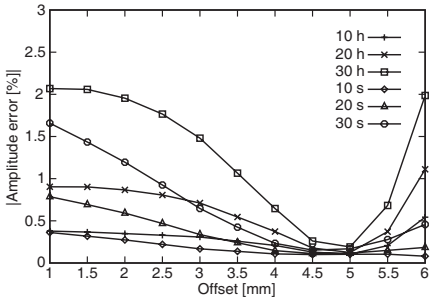

Figure 12. S_{11} amplitude error for half-height WR90 waveguides. $t = 1.27\,\text{mm}$; $h = 0.165\,\text{mm}$, $\varepsilon_r = 2.05$.

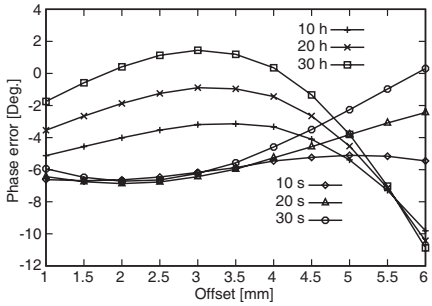

Figure 13. S_{11} phase error for half-height WR90 waveguides. $t = 1.27\,\text{mm}$; $h = 0.165\,\text{mm}$, $\varepsilon_r = 2.05$.

In Figures 10, 11, 12 and 13, we show the same graphs as in Figures 6, 7, 8 and 9 but with half-height WR90 waveguides ($a = 22.86\,\text{mm}$, $b = 5.08\,\text{mm}$). The effect of the higher-order modes interaction is almost the same for the radiating slots voltage error but is much reduced for the S_{11}.

We have also computed the voltage error for a spacing of $\frac{3}{4}\lambda_g$ between the radiating slots, getting a value of about 0.2° on the phase and less than 0.1% on the amplitude. The difference in the reflection coefficient in the feeding guide has been computed, too, but it is negligible (less than 2° on the phase, less than 0.1% on the amplitude), at least for the case considered here. As a consequence, only the offset and length of the two radiating slots closest to the coupling one need

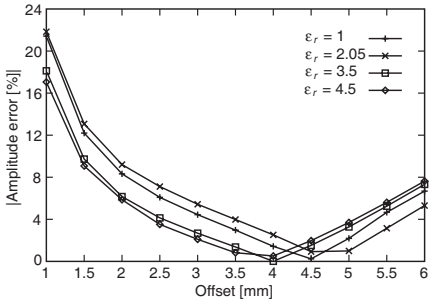

Figure 14. Amplitude error on the slot voltage for standard WR90 waveguides. $\theta = 20°h$; $t = 1.27\,\text{mm}$; $h = 0.165\,\text{mm}$.

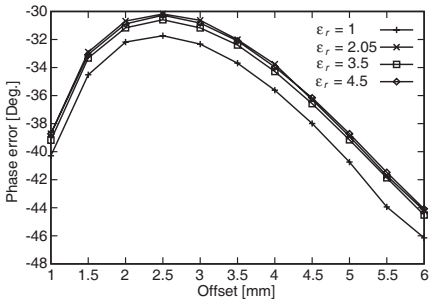

Figure 15. Phase error on the slot voltage for standard WR90 waveguides. $\theta = 20°h$; $t = 1.27\,\text{mm}$; $h = 0.165\,\text{mm}$.

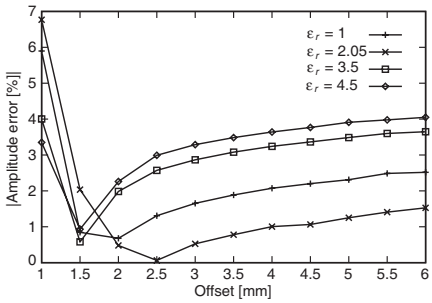

Figure 16. Amplitude error on the slot voltage for standard WR90 waveguides. $\theta = 20°s$; $t = 1.27\,\text{mm}$; $h = 0.165\,\text{mm}$.

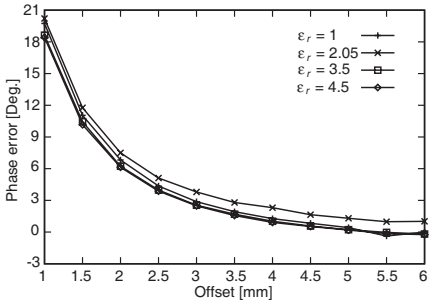

Figure 17. Phase error on the slot voltage for standard WR90 waveguides. $\theta = 20°s$; $t = 1.27\,\text{mm}$; $h = 0.165\,\text{mm}$.

to be modified to take into account this interaction in the design of a dielectric-covered slot array.

The effect of the variation of the dielectric cover permittivity has been evaluated. In Figures 14, 15, 16 and 17 we show the radiating slot voltage errors for different dielectric cover permittivity for standard WR90 waveguides.

Finally, in order to quantify the importance of an accurate evaluation of the array aperture distribution and to demonstrate the usefulness of the error curves presented in this section, we have designed a 16-element linear array with a $-30\,\text{dB}$ Chebychev distribution on a standard WR90 waveguide. The design frequency is 10 GHz; the coupling slot tilt angle is 30° with a soft orientation

(Figure 5); the slots width and dielectric cover parameters are the same as in Figure 6. The array has been synthesized with the procedure proposed in [12], which neglects the higher-order mode interaction between the coupling and the radiating slots. The simulated far field pattern of the designed array is shown in Figure 18. One can easily see that this array is far from the design requirements of −30 dB sidelobes. Actually, Figures 6 and 7 show that the two slots closer to the array center have an amplitude error of 0.7% and a phase error of 12° (since their offset is ±4.41 mm, as shown in Figure 18). Such errors are responsible for the degradation of the far field pattern.

In order to compensate these errors we can use our MoM analysis technique, and, by means of a trial and error procedure, we obtain that the 12° phase error can be compensated by increasing the normalized length of the two slots from 0.950 to 0.962. The slots offset does not need to be modified since the amplitude error is virtually zero. The far field pattern of the array with the corrected slots length is shown in Figure 18 and, as expected, demonstrates a significant improvement of the side lobe level (form −24 dB to −29 dB), which is almost at the design level.

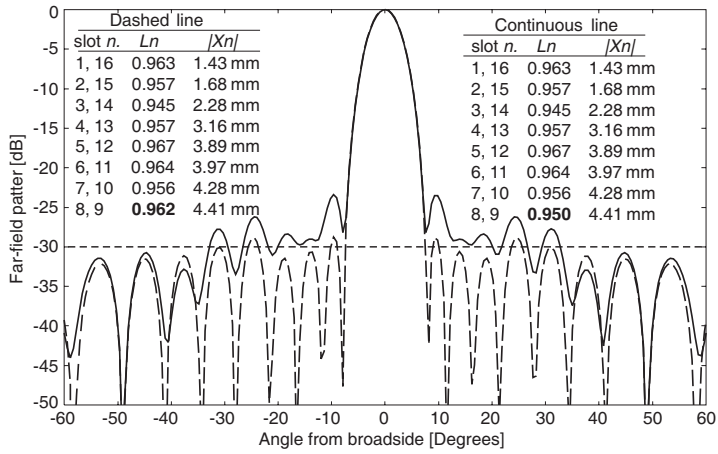

Figure 18. Far field pattern of a −30 dB Chebychev distribution linear array. The slots lengths Ln (normalized to half the free space wavelength) and offsets Xn of the designed arrays are shown in the tables. Continuous line: Design without higher order modes interaction. Dashed line: Design with the correction of the slots length described in the text.

5. CONCLUSION

An accurate technique to model the higher-order modes interaction between coupling and dielectric-covered radiating slots has been presented. It is based on the Method of Moments in the Galerkin formulation, which allows accurate and effective analysis. We show that the effect of the higher-order modes interaction between the coupling slot and the two nearest radiating slots cannot be neglected in the slot array design. The dielectric cover effect must be accurately taken into account because it strongly modifies the field and circuital properties of the slot array.

REFERENCES

1. Elliott, R. S., "An improved design procedure for small arrays of shunt slots," *IEEE Trans. Antennas Propagat.*, Vol. 31, 48–53, 1983.
2. Elliott, R. S. and W. R. O'Loughlin, "The design of slot arrays including internal mutual coupling," *IEEE Trans. Antennas Propagat.*, Vol. 34, 1149–1154, 1986.
3. Mazzarella, G. and G. Panariello, "Evaluation of the edge effects in slot arrays using the geometrical theory of diffraction," *IEEE Trans. Antennas Propagat.*, Vol. 37, 392–395, 1989.
4. Rengarajan, R. S. and G. M. Shaw, "Accurate characterization of coupling junctions in waveguide-fed planar slot arrays," *IEEE Trans. Microwave Theory Technique*, Vol. 42, 2239–2247, 1994.
5. Katehi, P. B., "Dielectric-covered waveguide longitudinal slots with finite wall thickness," *IEEE Trans. Antennas Propagat.*, Vol. 38, 1039–1045, 1990.
6. Mazzarella, G. and G. Montisci, "A rigorous analysis of dielectric-covered narrow longitudinal shunt slots with finite wall thickness," *Electromagnetics*, Vol. 19, 407–418, 1999.
7. Mazzarella, G. and G. Montisci, "Full-wave analysis of dielectric-covered radiating series slots," *Microwave and Optical Technology Letters*, Vol. 20, 67–72, 1999.
8. Mondal, M. and A. Chakraborty, "Resonant length calculation and radiation pattern synthesis of longitudinal slot antenna in rectangular waveguide," *Progress In Electromagnetics Research Letters*, Vol. 3, 187–195, 2008.
9. Mazzarella, G. and G. Montisci, "Wideband equivalent circuit of a centered-inclined waveguide slot coupler," *Journal of*

Electromagnetic Waves and Applications, Vol. 14, No. 1, 133–151, 2000.

10. Casula, G. A., G. Mazzarella, and G. Montisci, "Effective analysis of a microstrip slot coupler," *Journal of Electromagnetic Waves and Applications*, Vol. 18, No. 9, 1203–1217, 2004.
11. Zawadzki, M., S. Rengarajan, R. E. Hodges, and J. Chen, "Lowsidelobe slot arrays for the Juno microwave radiometer," *IEEE Antennas and Propagat. Society Int. Symp.*, Vol. 1, 1–4, 2010.
12. Casula, G. A. and G. Montisci, "Design of dielectric-covered planar arrays of longitudinal slots," *IEEE Antennas and Wireless Propagation Letters*, Vol. 8, 752–755, 2009.